

The dynamics crossover region in phenol- and cresol-phthalein-dimethylethers under different conditions of pressure and temperature

Riccardo Casalini^{1,3}, Marian Paluch^{1,2} and C Michael Roland¹

¹ Naval Research Laboratory, Chemistry Division, Code 6120, Washington, DC 20375-5342, USA

² Institute of Physics, Silesian University, Uniwersytwcka 4, 40-007, Poland

E-mail: casalini@ccs.nrl.navy.mil

Received 29 October 2002

Published 10 March 2003

Online at stacks.iop.org/JPhysCM/15/S859

Abstract

Dielectric relaxation times over a broad range of temperature and pressure for the glass former phenolphthalein-dimethylether (PDE) reveal a change of dynamics at a characteristic relaxation time τ_B . The value of τ_B was found to be largely insensitive to the particular combination of pressure and temperature of the measurement. Data for a second glass former, cresolphthalein-dimethylether, having a molecular structure very close to that of PDE, were also analysed. In this case, τ_B is much smaller, so the change of dynamics could not be observed in the elevated pressure experiments. The PDE data were in good agreement with the Adam–Gibbs model near T_g ($\tau > \tau_B$), while deviating for $\tau < \tau_B$. Finally, a possible connection between the observed T_B and theoretical models is presented.

1. Introduction

The evolution of a liquid into a glass, which typically happens during cooling, is a process whose nature is still much debated. The understanding of this evolution promises a better understanding of the glassy state itself, which due to its very slow but continuous change (requiring measuring times much longer than the average lifetime of a researcher) is a very difficult problem.

In recent years much attention has been concentrated on temperatures about 20% higher than T_g , at which several phenomena have been observed [1]: breakdown of both the Stokes–Einstein relation between the viscosity and translational diffusion [2, 3] and the Debye–Stokes–Einstein relation between the viscosity and orientational relaxation [4, 5], the loss of ergodicity as predicted by mode-coupling theory (MCT) [6], a broadening of the structural relaxation

³ Author to whom any correspondence should be addressed.

function [7, 8], a marked change in temperature dependence of the nanopore (unoccupied volume) radius [9], and splitting of the high-temperature relaxation into a slow process, with a relaxation time (τ) which diverges at T_g , and a faster relaxation, exhibiting Arrhenius behaviour through temperatures well below T_g . The change in dynamics reflected by these phenomena can be seen directly from analysis of the τ , viscosity, or conductivity of supercooled liquids. Derivatives of these quantities exhibit a break at a temperature corresponding to that at which the aforementioned phenomena transpire [3, 10, 11].

From the theoretical point of view, the temperature, T_B , at which these phenomena occur is often interpreted as the critical temperature T_c of MCT, which in its original version [1] predicts a divergence at T_c of relaxation time and viscosity, which is not observed experimentally. This failing is ascribed to an assumed crossover from liquid-like to hopping dynamics, the latter not included in MCT. Alternatively, in the landscape model [12], T_B is regarded as the temperature at which the dynamics becomes landscape dominated [13]. In the coupling model (CM) [14], the crossover observed at T_B is interpreted as a strong increase of the degree of intermolecular cooperativity [15]. T_B also recalls the (now discredited [16]) liquid–liquid transition postulated many years ago from the viscoelastic behaviour of polymers [17, 18].

While a typical experiment is done varying the temperature at atmospheric pressure, a more complete picture can be obtained when the dynamics is studied in all of pressure–temperature space [19], allowing an assessment of the influence of changes in density on the dynamics [20–24].

Herein, we describe evidence of a change of dynamics in glass formers above the glass transition for different conditions of temperature and pressure. Moreover, we show that the observed crossover is correlated with a deviation from the Adam–Gibbs (AG) model. These findings provide insight into the roles of different thermodynamic variables in the observed crossover. Finally, a possible connection between the observed crossover temperature and the critical temperature of the MCT is discussed, comparing the results for phenolphthalein-dimethylether (PDE) with previous findings for OTP.

2. Experimental details

Dielectric spectroscopy was carried out on two glass-forming liquids, having simple molecular structures and a resistance to crystallization: PDE and cresol-phthalein-dimethylether (KDE), the latter differing from PDE by the presence of a methyl group on each phenyl ring. The sample was synthesized in the laboratory of Professor H Sillescu and obtained from Dr Roland Böhmer of Johannes Gutenberg Universität, Mainz, Germany. The glass transition temperatures of the two materials are $T_g = 298$ K for PDE and 312 K for KDE. Spectra were acquired over ten decades of frequency, with variation of either pressure or temperature; a detailed description of the apparatus can be found elsewhere [25]. Some of the data for KDE were reported in a previous publication [26]. The samples were in the liquid state (i.e., above the pressure-dependent T_g) during all measurements. The data for atmospheric pressure were compared with those of Stickel [27], and found to be in good agreement. Thus, we present only the latter since they have a more extended range. The relaxation time, defined from the frequency of the dielectric loss peak, corresponds approximately to the most probable relaxation time. For the materials investigated herein, no secondary relaxation was evident.

3. Results

3.1. PDE

In figure 1 we display the relaxation times for PDE versus inverse temperature (figure 1(a)) and versus pressure (figure 1(b)) at five fixed temperatures above the atmospheric pressure T_g .

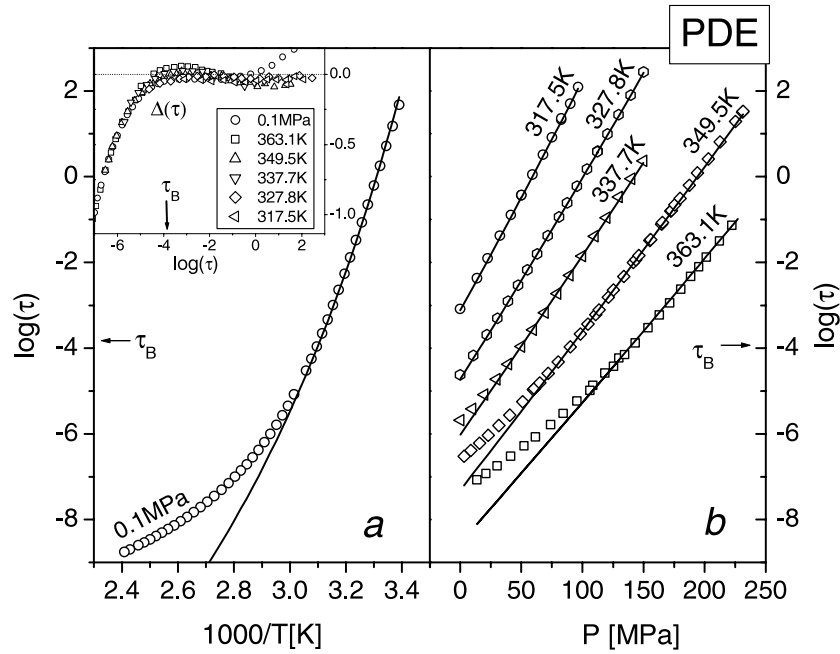


Figure 1. Dielectric relaxation time data for PDE. (a) τ versus inverse temperature from [34] at atmospheric pressure; (b) τ versus pressure at fixed temperatures indicated in the plot. Solid lines are the best fit to the AG model. In the inset we show the difference $\Delta(\tau) = \log(\tau) - \log(\tau_{AG})$ versus $\log(\tau)$, where τ_{AG} is the best fit using the AG model.

A strong sensitivity of the relaxation time to both pressure and temperature is evident, making this material very suitable for this study.

To reveal the change of dynamics at high temperature, Stickel *et al* [27] proposed the use of the function $\phi_T = (d(\log(\tau))/d(1000/T))^{-\frac{1}{2}}$. Vogel–Fulcher (VF) behaviour is often observed near T_g [28, 29]:

$$\tau = \tau_0 \exp\left(\frac{DT_0}{T - T_0}\right) \quad (1)$$

where T_0 is the Vogel temperature, D is the fragility parameter, and τ_0 is the relaxation time in the limit of high temperatures. The function ϕ_T is very useful for evidencing deviation from this behaviour because it transforms a VF into a linear dependence with respect to inverse temperature. From calculating ϕ_T for PDE, we determined a change of slope at $\tau_B \sim 10^{-4}$ s [30]. We consider that the pressure behaviour of τ in the proximity of the glass transition can be well described by a VF-like equation [31, 32]:

$$\tau(P) = \tau_P \exp\left(\frac{D_P P}{P_0 - P}\right), \quad (2)$$

where P is the pressure, τ_P can be obtained from isobaric data at atmospheric pressure, P_0 denotes the pressure at which τ diverges, and D_P can be referred to, for consistency, as the pressure fragility parameter [33]. Consequently, a function similar to ϕ_T can be defined: $\phi_P = (d(\log(\tau))/dP)^{-\frac{1}{2}}$. The function ϕ_P is calculated for the four isotherms. At higher temperature there is a clear change in the pressure dependence [30]. The value of the relaxation time corresponding to this change is $\tau_B \sim 10^{-4}$ s, equivalent to the value at atmospheric pressure [34]; that is, τ_B is independent of temperature and pressure.

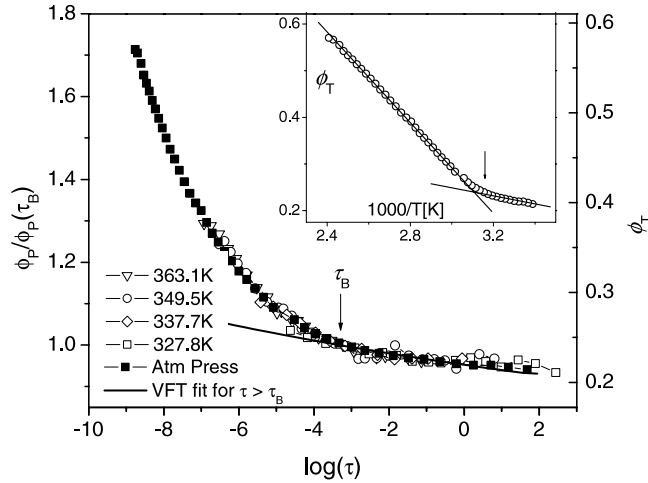


Figure 2. ϕ_P calculated for the four isotherms (figure 1(a)) normalized by their value at τ_B , together with ϕ_T , with all functions plotted versus $\log(\tau)$. In the same figure, to evidence the deviation from a VF, we report also the ϕ_T calculated for the VF fit (valid for $\tau > \tau_B$). In the inset we show ϕ_T versus inverse temperature.

As further evidence that the pressure crossover has the same characteristic time as its temperature counterpart ϕ_T , we plot in figure 2 both functions $\log(\tau)$. In this figure we show the function ϕ_P calculated for the four isotherms at higher temperatures normalized by their value at τ_B , together with ϕ_T . Note that in the plots of ϕ_T and ϕ_P versus $\log(\tau)$, the VF behaviour is no longer linear; thus to evidence the deviation from a VF form, the ϕ_T calculated for the VF fit (valid for $\tau > \tau_B$) is also displayed. It is evident that the behaviour of the function ϕ_P is the same, and coincides with that of the Stickel function ϕ_T .

3.2. KDE

The dielectric relaxation times for KDE for varying temperatures at atmospheric pressure and varying pressures at $T = 364.6$ K are shown in figures 3(a) and (b) respectively. Like PDE, KDE has a strong pressure and temperature dependence. Comparing the pressure dependence of the glass transition temperature dT_g/dP (calculated at atmospheric pressure) and the steepness index $m = \left. \frac{d \log(\tau)}{d(T/T_g)} \right|_{T=T_g}$, we have for KDE $dT_g/dP = 307$ K GPa $^{-1}$ and $m = 72.5$ [26] and for PDE $dT_g/dP = 260$ K GPa $^{-1}$ and $m = 85$. Thus, KDE is more sensitive to pressure but less sensitive to temperature. This difference may seem surprising considering that their molecular structures are very close. However, the activation volume, $\Delta V (= RT \frac{\partial \log \tau}{\partial P})$ at T_g , which is proportional to the product of m and dT_g/dP [32]:

$$\Delta V(T_g) = \ln(10) R m \frac{dT_g}{dP} \quad (3)$$

where R is the gas constant, is equal to 420 cm 3 mol $^{-1}$ for both PDE and KDE. The similarity of their molecular structures is reflected in ΔV .

In figures 3(c) and (d) we display the functions $\phi_T(T)$ and $\phi_P(P)$ as calculated from the $\tau(T, P)$ data for KDE. From the ϕ_T behaviour it is evident that a change in the dynamics occurs at $\tau_B \sim 10^{-6}$ s, which is about a hundredfold smaller than τ_B for PDE. Our value of τ_B is lower than that reported in [26]. The data are the same, and the difference is due only to the

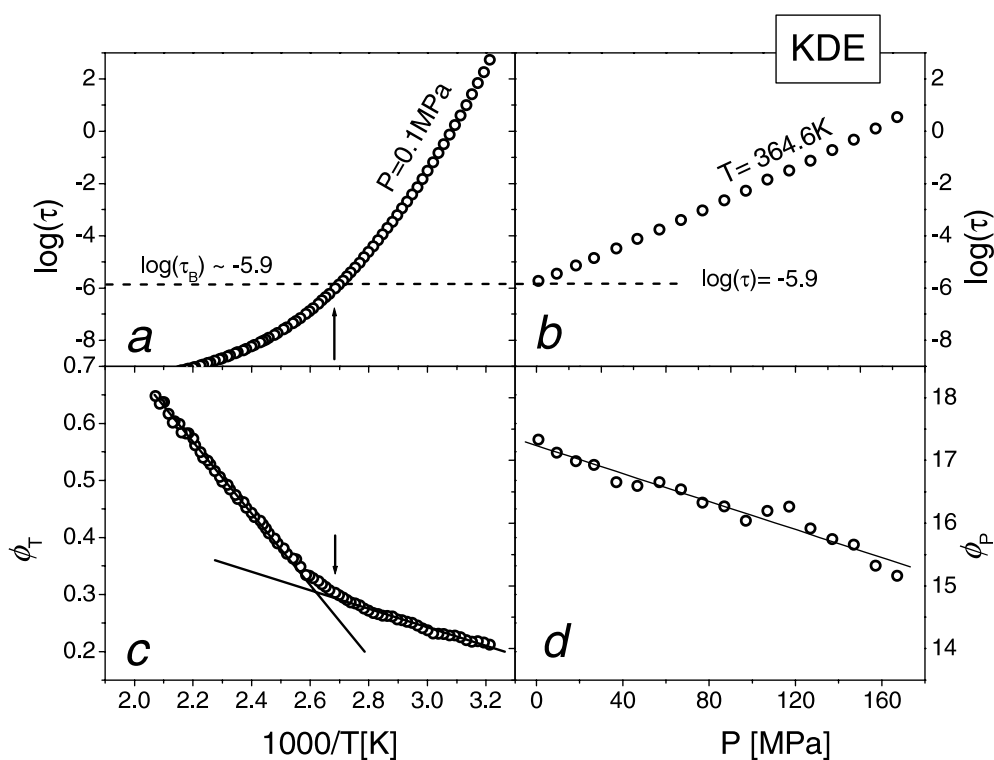


Figure 3. Dielectric relaxation time data for KDE: (a) τ versus inverse temperature from [34] at atmospheric pressure; (b) τ versus pressure at fixed temperature indicated in the plot; (c) the derivative function ϕ_T versus inverse temperature for data reported in (a); (d) the derivative function ϕ_P versus pressure for the data reported in (b).

different method used to determine T_B . No change in the slope of $\phi_P(P)$ is observed, since the pressure measurements cover only a limited range. This result is at least consistent with a constant $\tau_B(T, P)$. This comparison of KDE and PDE emphasizes that the value of $\tau_B(T, P)$ is not universal. It is striking that for materials having very similar molecular structures, τ_B differs by about two orders of magnitude.

4. Discussion

4.1. Test of the AG model

Of the different theoretical models proposed for interpreting the slowing down of the dynamics upon approach to the glass transition, much attention has been directed to the model of AG [35], which predicts

$$\tau = \tau_{AG} \exp\left(\frac{A}{TS_c}\right) \quad (4)$$

where S_c is the configurational entropy, A is a constant related to the intermolecular potential, and τ_{AG} is the relaxation time in the limit of high temperatures. The important result of this model is establishing a link between the dynamics (τ) and thermodynamical quantities (S_c). It is noteworthy that equation (4) has been found to be valid for simulations at short times [36, 37], which arise from a theoretical approach different to that used originally by AG.

The operative definition proposed by AG for determining S_c is considering it as equal to the excess entropy, S_{ex} , of the melt with respect to the crystal. However, as pointed out by Goldstein [38], this definition is problematic, because S_{ex} may include vibrational terms, with consequent overestimation of S_c . This point has recently been emphasized by Johari [39, 40] and Angell [41]. Nevertheless, tests of the AG model using S_{ex} have been successful for temperatures not too far from T_g [42–45], presumably reflecting at least proportionality between S_c and S_{ex} [41, 46], as found by computer simulations [47, 48].

Taking S_c equal to S_{ex} , the full pressure and temperature dependences can be written as

$$S_c(T, P) = \Delta S_{fus} + \int_{T_K}^T \frac{\Delta C_P(T')}{T'} dT' - \int_0^P \Delta \left(\frac{\partial V}{\partial T} \right)_{P'} dP' \quad (5)$$

where ΔS_{fus} is the entropy of fusion. The first integral is related to the excess molar heat capacity, $\Delta C_P = C_P^{melt} - C_P^{crystal}$, of the melt relative to the crystal, and the second integral can be expressed in terms of the excess molar thermal expansion, $\Delta \left(\frac{\partial V}{\partial T} \right)_P = \left(\frac{\partial \Delta V}{\partial T} \right)_P = \left(\frac{\partial (V^{melt} - V^{crystal})}{\partial T} \right)_P$. At atmospheric pressure ($P \sim 0$), the second integral is zero, and since the temperature dependence of the excess heat capacity can be described over a limited range by $\Delta C_P(T) = \kappa/T$, then $S_c(T) = S_\infty - \kappa/T$, where κ is a constant and S_∞ is the limit of S_c at very high temperatures [45]. On substituting this equation into equation (4), the VF expression is obtained, where T_0 is the Vogel temperature ($T_0 = \kappa/S_\infty$) and D ($D = C/\kappa$) is the fragility parameter. At pressures above atmospheric, the second integral of equation (5), describing the isothermal reduction of S_c , is non-negligible. On substituting equation (5) in (4), a VF-like equation for $\tau(T, P)$ is again obtained, with the Vogel temperature now defined as [49]

$$T_0^*(T, P) = \frac{T_0}{1 - \frac{1}{S_\infty} \int_0^P \Delta \left(\frac{\partial V}{\partial T} \right)_{P'} dP'} \quad (6)$$

At low pressures, the pressure dependence of the crystal thermal expansivity is negligible [49], and equation (6) can be rewritten as

$$T_0^*(T, P) = \frac{T_0}{1 + \frac{1}{S_\infty} \left[P \left(\frac{\partial V}{\partial T} \right)_{P=P_{atm}}^{cryst} - \int_0^P \left(\frac{\partial V}{\partial T} \right)_{P'}^{melt} dP' \right]} \quad (7)$$

in which the integral can be calculated if $V(T, P)$ for the melt is known. Accordingly, a function describing both the pressure and temperature dependence of τ according to equation (4) will require, together with the three VF parameters D , T_0 , and τ_0 for $P \sim 0$, two additional quantities S_∞ and $\left(\frac{\partial V}{\partial T} \right)_{P=P_{atm}}^{cryst}$. In favourable cases, these can be related to macroscopic physical properties of the material. Tests of the AG model have been previously carried out, using approximate values for $\left(\frac{\partial \Delta V}{\partial T} \right)_P$ [25, 49–51]. Herein, we execute a more accurate assessment, by calculating the integral of the thermal expansivity of the melt from $V(T, P)$ data [1, 51] for each condition of temperature and pressure.

The fit to equations (4) and (5) was carried out on both isobaric (one pressure) and isothermal (five temperatures) data. The analysis was limited to $\tau_B \sim \tau < 10^{-4}$ s because of the deviation from a single VF form evidenced from the Stickel plot (inset, figure 2). For $\tau < \tau_B$ in figure 1, a good agreement of the fit (solid lines) to the experimental data for all temperatures and pressures is evident. The best-fit parameters were $\log(\tau_0) = -20.7$, $D = 19.2$, $T_0 = 215$ K, $S_\infty = 112$ J K⁻¹ mol⁻¹, and $\left(\frac{\partial V}{\partial T} \right)_{P=P_{atm}}^{cryst} = 1.7 \times 10^{-4}$ cm⁻³ K⁻¹. The first three values are equal to those found previously for atmospheric pressure [34, 52]. The thermal expansivity obtained for the crystal is quite close to the value measured at $P = 10$ MPa, namely $\left(\frac{\partial V}{\partial T} \right)_{P=10 \text{ MPa}}^{cryst} = 1.9 \times 10^{-4}$ cm⁻³ K⁻¹ [51].

It is interesting that the best fits to the AG model (solid lines in figure 1(b)), which are nearly linear, show a clear deviation for short τ , similar to the deviation in the τ versus

Table 1. The expansion coefficient α and isothermal compressibility β for PDE at the T and P at which the change of dynamics is observed, and the calculated value of the expression in equation (8).

T (K)	P (MPa)	$\alpha \times 10^4$ (K $^{-1}$)	$\beta \times 10^4$ (MPa $^{-1}$)	$T_c \left(\frac{\beta}{dT/dP _{\tau=\tau_c}} - \alpha \right)$
318.9	0.1	6.2	4.0	0.26
327.8	30.4	5.8	3.7	0.25
337.7	66.2	5.4	3.4	0.23
349.5	108.5	5.0	3.0	0.21
363.1	160.7	4.7	2.7	0.19

temperature plot. To show this better, we plotted, in the inset to figure 1, the difference between the experimental points and the best fit to the AG model ($\Delta(\tau) = \log(\tau) - \log(\tau_{AG})$). The deviation for all data (both isobaric and isothermal) occurs at about the same relaxation time. This result recalls the deviations from the AG model observed for several materials from measurements at atmospheric pressure, in which S_c was calculated from calorimetric data [45, 53].

4.2. Comparison with other theoretical predictions

It is significant that the changes in dynamics shown herein have similarities to the behaviour reported for other glass formers, for example, ortho-terphenyl (OTP) [54]. In a recent review on OTP [55], Tölle showed that the temperature for the change in dynamics as determined using the Stickel function, $T_B \cong 290$ K at $\tau_B \sim 10^{-6}$ s [54], is very close to the critical temperature, T_c , of MCT [6]. More relevant, Tölle *et al* concluded, from measurements of the pressure and temperature dependence of the static structure factor [19, 55], that the structure factor does not change significantly along an isochronous line. This implies that the relaxation time at the dynamic singularity of MCT should be independent of pressure and temperature, analogous to the results herein for τ_B . However, the T_c of MCT corresponds to a transition that is not observed in relaxation data, and it remains to be established whether this can be identified with T_B .

To compare our results with the findings of Tölle for OTP, we verified the relationship that he proposed [55]:

$$T_c \left(\frac{\beta}{dT/dP|_{\tau=\tau_c}} - \alpha \right) \cong \frac{1}{4} \quad (8)$$

from MCT, which predicts and expresses the repulsive part of the potential. In equation (8), $\beta = -\frac{1}{V} \left(\frac{\partial V}{\partial P} \right)_T$ is the isothermal compressibility and $\alpha = \frac{1}{V} \left(\frac{\partial V}{\partial T} \right)_P$ is the thermal expansion coefficient. Considering $T_c = T_B$ and $\tau_c = \tau_B$, we calculate the values of α and β from $V(T, P)$ measurements on PDE [51], together with the value of the expression in equation (8). The results, reported in table 1, are very close to the expected values. The deviation from the predicted value of 0.25 is of the order observed by Tölle for OTP [55]: 0.23 ± 0.03 for PDE versus 0.26 ± 0.03 for OTP [55].

In the framework of the CM [14], the constancy of τ_B is consistent with the observed constancy of the shape of the dielectric relaxation spectra at the same relaxation time for different conditions of T and P [25, 26]. Thus, the expected correlation of the crossover with the strong increase in the severity of intermolecular cooperativity is borne out by the results herein.

5. Conclusions

Evidence of a change of dynamics in PDE under different conditions of temperature and pressure is reported. We observe that for very different values of T and P , the change of dynamics transpires at the same relaxation time, $\tau_B \sim 10^{-4}$ s. To show this more clearly, we make use of the Stickel function ϕ_T and of its pressure counterpart ϕ_P to obtain the master curves in figure 2. It is worth noting that we observed the same behaviour, with $\tau_B(T, P) = \text{constant}$, for two other materials, and in these cases also, τ_B was found to be dependent on the material [25, 30].

Data for a second glass former (KDE) having a molecular structure very similar to that of PDE were also analysed. In this case, τ_B is much smaller, so the change of dynamics could not be observed in the elevated pressure experiments. Evidently, τ_B , while constant for a given chemical species, is not universal.

An analysis of PDE data using the AG model was carried out taking into account the $V(T, P)$ dependence. The model was found to describe accurately the τ -behaviour in the proximity of T_g for $\tau > \tau_B$, while a deviation from the AG prediction is observed in both the temperature and pressure data for $\tau < \tau_B$.

Finally, a possible connection between the observed T_B and the critical temperature of the MCT is discussed. The results for PDE are compared with previous findings for OTP.

Acknowledgments

This work was supported by the Office of Naval Research. The authors thank K L Ngai, W Götze and F Sciortino for stimulating discussions and J J Fontanella for experimental assistance. M Paluch also thanks the Committee for Scientific Research, Poland (KBN, grant No 2PO3B 033 23), for financial support.

References

- [1] Angell C A, Ngai K L, McKenna G B, McMillan P F and Martin S W 2000 *J. Appl. Phys.* **88** 3113
- [2] Ediger M D, Angell C A and Nagel S R 1996 *J. Phys. Chem.* **100** 13200
- [3] Ngai K L, Magill J H and Plazek D J 2000 *J. Chem. Phys.* **112** 1887
- [4] Chang I and Sillescu H 1997 *J. Phys. Chem. B* **101** 8794
- [5] Comez L, Fioretto D, Palmieri L, Verdini L, Rolla P A, Gapinski J, Pakula T, Patkowski A, Steffen W and Fischer E W 1999 *Phys. Rev. E* **60** 3086
- [6] Götze W and Sjogren L 1992 *Rep. Prog. Phys.* **55** 241
- [7] Ngai K L 1999 *J. Phys. Chem. B* **103** 5895
- [8] Ngai K L and Roland C M 2002 *Polymer* **43** 567
- [9] Ngai K L, Bao L R, Yee A F and Soles C L 2001 *Phys. Rev. Lett.* **87** 215901
- [10] Stickel F, Fischer E W and Richert R 1995 *J. Chem. Phys.* **102** 6251
- [11] Magill J H and Plazek D J 1966 *J. Chem. Phys.* **45** 3038
- [12] Stillinger F H 1995 *Science* **267** 1935
- [13] DeBenedetti P G and Stillinger F H 2001 *Nature* **410** 259
- [14] Ngai K L 1979 *Comment. Solid State Phys.* **9** 121
Tsang K Y and Ngai K L 1996 *Phys. Rev. E* **54** R3067
Tsang K Y and Ngai K L 1997 *Phys. Rev. E* **56** R17
- [15] Ngai K L 1999 *J. Chem. Phys.* **111** 3639
- [16] Plazek D J 1982 *J. Polym. Sci., Polym. Phys. Edn* **20** 1533
Plazek D J and Gu G F 1982 *J. Polym. Sci., Polym. Phys. Edn* **20** 1551
Chen J, Kow C, Fetters L J and Plazek D J 1982 *J. Polym. Sci., Polym. Phys. Edn* **20** 1565
Orbon S J and Plazek D J 1982 *J. Polym. Sci., Polym. Phys. Edn* **20** 1575
- [17] Boyer R F 1985 *J. Polym. Sci., Polym. Phys. Edn* **23** 21
- [18] Boyer R F 1963 *Rubber Chem. Technol.* **36** 1303

- [19] Tölle A, Schober H, Wuttke J, Randl O G and Fujara F 1998 *Phys. Rev. Lett.* **80** 2374
- [20] Ferrer M L, Lawrence Ch, Demirjian B G, Kivelson D, Alba-Simonesco Ch and Tarjus G 1998 *J. Chem. Phys.* **109** 8010
- [21] Paluch M, Casalini R and Roland C M 2002 *Phys. Rev. B* **66** 092202
- [22] Paluch M, Roland C M, Casalini R, Meier G and Patkowski A 2003 *J. Chem. Phys.* **118** at press
- [23] Paluch M, Casalini R, Hensel-Bielowka S and Roland C M 2002 *J. Chem. Phys.* **116** 9839
- [24] Hensel-Bielowka S, Paluch M and Roland C M 2003 *J. Phys. Chem. B* **106** 12459
- [25] Casalini R, Paluch M, Fontanella J J and Roland C M 2002 *J. Chem. Phys.* **117** 4091
- [26] Paluch M, Ngai K L and Hensel-Bielowka S 2001 *J. Chem. Phys.* **114** 10872
- [27] Stickel F, Fischer E W and Richert R 1996 *J. Chem. Phys.* **104** 2043
- [28] Vogel H 1921 *Z. Phys.* **222** 645
- [29] Fulcher G S 1923 *J. Am. Ceram. Soc.* **8** 339
- [30] Casalini R, Paluch M and Roland C M *J. Chem. Phys.* submitted
- [31] Johari G P and Whalley E 1972 *Faraday Symp. Chem. Soc.* **6** 23
- [32] Paluch M, Gapinski J, Patkowski A and Fischer E W 2001 *J. Chem. Phys.* **114** 8048
- [33] Hodge I M 1996 *J. Non-Cryst. Solids* **202** 164
- [34] Stickel F 1995 *Thesis Johannes Gutenberg-Universität Mainz*
- [35] Adam G and Gibbs J H 1965 *J. Chem. Phys.* **43** 139
- [36] Sastry S 2001 *Nature* **409** 164
- [37] Sciortino F, Kob W and Tartaglia P 1999 *Phys. Rev. Lett.* **83** 3214
- [38] Goldstein M 1975 *J. Chem. Phys.* **64** 4767
- [39] Johari G P 2000 *J. Chem. Phys.* **112** 8958
- [40] Johari G P 2002 *J. Non-Cryst. Solids* **307–310** 387
- [41] Angell C A and Borick S 2002 *J. Non-Cryst. Solids* **307–310** 393
- [42] Magill J H 1967 *J. Chem. Phys.* **47** 4802
- [43] Takahara S, Yamamuro O and Suga H 1994 *J. Non-Cryst. Solids* **171** 259
- [44] Takahara S, Yamamuro O and Matsuo T 1995 *J. Phys. Chem.* **99** 9580
- [45] Richert R and Angell C A 1998 *J. Chem. Phys.* **108** 9016
- [46] Martinez L M and Angell C A 2000 *Nature* **410** 663
- [47] Starr F W, Sastry S, LaNave E, Scala A, Stanley H E and Sciortino F 2001 *Phys. Rev. E* **63** 041201
- [48] Kamath S, Colby R H, Kumar S K and Bashnagel J 2002 *J. Chem. Phys.* **116** 865
- [49] Capaccioli S, Lucchesi M, Casalini R, Presto S, Rolla P A, Vicioso M T, Corezzi S and Fioretto D 2002 *Phil. Mag. B* **82** 652
- [50] Casalini R, Lucchesi M, Capaccioli S, Rolla P A and Corezzi S 2001 *Phys. Rev. E* **63** 031207
- [51] Paluch M, Casalini R, Best A and Patkowski A 2002 *J. Chem. Phys.* **117** 7624
- [52] Patkowski A, Paluch M and Kriegs H 2002 *J. Chem. Phys.* **117** 2192
- [53] Ngai K L 1999 *J. Phys. Chem. B* **103** 5895
- [54] Hansen C, Stickel F, Berger T, Richert R and Fischer E W 1997 *J. Chem. Phys.* **107** 1086
- [55] Tölle A 2001 *Rep. Prog. Phys.* **64** 1473